Charge-density-wave formation in $TiSe_2$ driven by an incipient antiferroelectric instability

2002 J. Phys.: Condens. Matter 14 7973

(http://iopscience.iop.org/0953-8984/14/34/316)

INSTITUTE OF PHYSICS PUBLISHING JOURNAL OF PHYSICS: CONDENSED MATTER

J. Phys.: Condens. Matter **14** (2002) 7973–7979 PII: S0953-8984(02)34493-X

Charge-density-wave formation in $TiSe_2$ driven by an incipient antiferroelectric instability

Annette Bussmann-Holder[1] **and Helmut Büttner**[1,2]

[1] Max-Planck-Institut für Festkörperforschung, Heisenbergstr. 1, D-70569 Stuttgart, Germany
[2] Lehrstuhl für Theoretische Physik I, Universität Bayreuth, D-95440 Bayreuth, Germany

Received 4 March 2002
Published 15 August 2002
Online at stacks.iop.org/JPhysCM/14/7973

Abstract

Recently reported temperature-dependent synchrotron x-ray thermal diffuse scattering data (Holt M, Zschack P, Hong H, Chou M Y and Chiang T C 2001 *Phys. Rev. Lett.* **86** 3799) are analysed within an anharmonic electron–phonon interaction model, where the observed zone boundary phonon softening is related to an incipient antiferroelectric instability. The parameter-free model reproduces the temperature dependence of the soft phonon mode in excellent agreement with the experimental data. Predictions for the charge-density-wave-induced gap are made and consequences for the electronic structure changes are discussed.

(Some figures in this article are in colour only in the electronic version)

Charge-density-wave (CDW) formation has been studied extensively theoretically as well as experimentally [1] since it is thought to be a prototypical consequence of electron–phonon interaction effects. Besides the Pt-based one-dimensional conductors [2], the layered transition metal dichalcogenides are also systems where the formation of CDWs has been explored thoroughly by various experimental techniques [1, 3]. While frequently incommensurate CDWs are reported, $TiSe_2$ and analogues undergo a transition to a commensurate CDW state with doubling of the lattice constants [4] and phonon softening [5–7]. Even though $TiSe_2$ has been studied by means of various experimental tools during the last few decades, no direct evidence for phonon softening in connection with CDW formation has been obtained until recently, when temperature-dependent synchrotron x-ray thermal diffuse scattering experiments revealed that the CDW formation is intimately tied to the condensation of a zone boundary phonon mode [8]. These new results yield important information about the microscopic mechanism of the CDW state, which was speculated to be due to exciton formation [9–11], band Jahn–Teller effects [3, 12] or the suppression of an antiferroelectric transition due to carriers [10]. Various lattice dynamical calculations [7, 13] have been performed for $TiSe_2$ to reproduce the few experimental results on the phonon dispersion and/or the Raman scattering data. Also in [8] the earlier model parameters have been used in order to

model the new data and a fitting to the experimental temperature dependence has been carried through to mimic the zone boundary mode softening.

In the following we will show that these new experiments can be reproduced without any fitting parameters by using a nonlinear electron–phonon interaction scheme, which typically can be applied to model ferroelectric phase transitions [14–17]. We use this specific model to calculate the dynamical properties of $TiSe_2$ because the experimental data are astonishingly reminiscent of those for antiferroelectric systems, which can be understood in terms of the above model by folding back the soft zone boundary mode to the zone centre [16]. Of course we are aware of the fact that this modelling does not capture the full band structure complexity, but we assume that the main effects of charge ordering are related to the rearrangements of the Se-related p electrons and the superlattice formation. This assumption is strongly supported by results from *ab initio* band structure calculations which have shown that a single structural parameter controls the electronic properties [18]. Phenomenologically, the lattice dynamical model is a nonlinear shell model representation where the nonlinearity is located at the chalcogenide-ion lattice site, since these doubly negatively charged ions are unstable as free ions [19]. The relevant dynamics of $TiSe_2$ stems from displacement patterns which are a superposition of three distortion waves [5]. This superposition allows one to represent the corresponding dynamical pattern along the relevant crystallographic direction within a pseudo-one-dimensional array, where only a transverse optical mode has to be considered. The corresponding Hamiltonian reads [15]

$$H = \tfrac{1}{2}\sum_n [m_i \dot{u}_{in}^2 + m_e \dot{v}_{1n}^2] + \tfrac{1}{2}\sum_n [f'(u_{1n} - u_{1n+1})^2 + f(u_{2n} - v_{1n})^2 + f(u_{2n+1} - v_{1n})^2] + \tfrac{1}{2}\sum_n [g_2(v_{1n} - u_{1n})^2 + \tfrac{1}{2}g_4(v_{1n} - u_{1n})^4]. \tag{1}$$

Here m_i ($i = 1, 2$; $1 = \mathrm{Se}$, $2 = \mathrm{Ti}$) are the ionic masses with displacement coordinate u, and v is the Se-related electronic shell displacement coordinate. While the coupling f of the Se shell to the nearest-neighbour Ti core is harmonic, the on-site core–shell coupling at the Se lattice site consists of a harmonic term, g_2, and an anharmonic one, g_4. In ferroelectrics these two terms typically have opposite sign, g_2 being attractive while g_4 is repulsive, thus creating a local double-well potential. This is not necessarily true for other compounds where the signs of both couplings have to be determined self-consistently. However, independently of the signs of g_2, g_4, stability of the system is in each case guaranteed by the next-nearest-neighbour coupling constant f'. Treating the shell motion within the adiabatic approximation and introducing a relative core–shell displacement coordinate $w = v - u$ at the Se lattice site, the third-power term in w, which appears in the equations of motion, can be replaced by a cumulant expansion such as $g_2 w + g_4 w^3 = w(g_2 + 3g_4\langle w^2\rangle_T) = g_T w$, where $\langle w^2\rangle_T$ is the thermal average over the relative core–shell displacement coordinate which has to be determined self-consistently via $g_T(q) = g_2 + 3g_4 \sum_{q,j} \frac{\hbar}{\omega(q,j)} w^2(q, j) \coth \frac{\hbar\omega(q,j)}{2kT}$, where the frequencies are dependent on momentum q and branch j, and g_T becomes a function of momentum and branch as well. The equations of motion obtained from equation (1) and using the above definition for $g_T(q) \cong g_T$ read

$$\begin{aligned} -m_1\omega^2 U_1 &= -[4f' \sin^2(qa) + 2\tilde{f}]U_1 + 2\tilde{f}\cos(qa)U_2 \\ -m_2\omega^2 U_2 &= -\left[\frac{4f\,\tilde{f}}{g_T}\sin^2(qa) + 2\tilde{f}\right]U_2 + 2\tilde{f}\cos(qa)U_1 \end{aligned} \tag{2}$$

where the shell displacement has been treated in the adiabatic approximation, $\tilde{f} = f g_T/(2f + g_T)$ and U_1, U_2 are the eigenvectors. The resulting lattice mode frequencies, which enter the definition of g_T, are given by

$$\omega_{1,2}^2 = \frac{1}{2m_1}[4f'\sin^2(qa) + 2\tilde{f}] + \frac{1}{2m_2}\left[\frac{4f\ \tilde{f}}{g_T}\sin^2(qa) + 2\tilde{f}\right] \pm \left\{\left[\frac{1}{2m_1}\left[4f'\sin^2(qa) + 2\tilde{f}\right] - \frac{1}{2m_2}\left[\frac{4f\ \tilde{f}}{g_T}\sin^2(qa) + 2\tilde{f}\right]\right]^2 + \frac{1}{m_1 m_2}4\tilde{f}^2\cos(qa)\right\}^{1/2}. \quad (3)$$

Since the lattice constants of $TiSe_2$ double upon CDW formation, we fold—in a similar manner to antiferroelectrics—the acoustic branch back to the zone centre and fix the involved parameters f, f' through the experimentally given zone boundary frequencies; i.e. $\omega_{TA}^2(q = 2\pi/a) = (1/m_1)[4f' + 2fg_T/(2f + g_T)]$ and $\omega_{TO}^2(q = 2\pi/a) = 2f/m_2$. The on-site harmonic and anharmonic core–shell couplings have to be determined self-consistently through the constraint that $g_T = 0$ at the CDW transition temperature T_c. This corresponds to the following constraint for the core–shell interactions:

$$\frac{|g_2|}{3g_4} = \sum_{q,j}\frac{\hbar}{\omega(q,j)}w^2(q,j)\coth\frac{\hbar\omega(q,j)}{2kT_c} \quad (4)$$

with ω as defined by equation (3). Since the definition of g_T is valid at all temperatures, a single set of core–shell coupling constants is obtained. The parameters, as derived from experiment together with the self-consistently derived electron–phonon couplings, are of the same order as in ferroelectrics and are listed in table 1. In figure 1 we show a comparison of the experimental and theoretical data for the frequency of the soft zone boundary mode as a function of temperature for both regimes, the 'paraelectric' and the CDW state. Obviously an extremely convincing agreement between theory and experiment is achieved by our theoretical modelling. Since the data below T_c are an extrapolation of the high-temperature data and do not correspond to actual measurements [8], we consider our slightly different theoretical results as a challenge to experimentalists to test this regime for temperature dependence of the soft mode. Even though early Raman measurements [20] already looked into the CDW state, the experimental resolution seems unsatisfactory to us for comparing the results with our modelling. In agreement with [8], the scattering intensity variation with temperature is obtained mainly through the weight of the low-frequency mode at the zone boundary and is approximately proportional to $1/\omega^2$. In figure 2 we show our results which compare astonishingly well with the data of [8] shown therein in figure 2. Similarly we are able to predict the dispersion of the soft zone boundary mode, but in contrast to previous calculations [7, 8, 13], not by fitting the parameters with variations of temperature, but by using the self-consistent method outlined above. In figure 3 we compare our model predictions with previous ones [8] and observe again an extremely good agreement.

The question which arises here is—of course—how can this scenario, based on an incipient antiferroelectric phase transition, be related to the low-temperature CDW state? As outlined above, the rearrangement of the Se p electrons is modelled by an effective electron–phonon interaction Hamiltonian where the coupling strength g_T is determined by the above-derived self-consistent procedure. It is important to note here that the magnitude of the relative core–shell displacement coordinate w determines the degree of electron localization/delocalization where the limit $w \to \infty$ corresponds to complete ionization, while for $w \to 0$ the dipole moment is constant. Obviously neither of these limiting cases applies here, but the temperature-dependent changes in w indicate the degree of electronic redistribution introduced through the coupling to the lattice. These redistributions are frozen in at T_c and give rise to the charge-density-wave formation below T_c. In analogy to [2], the corresponding Hamiltonian reads

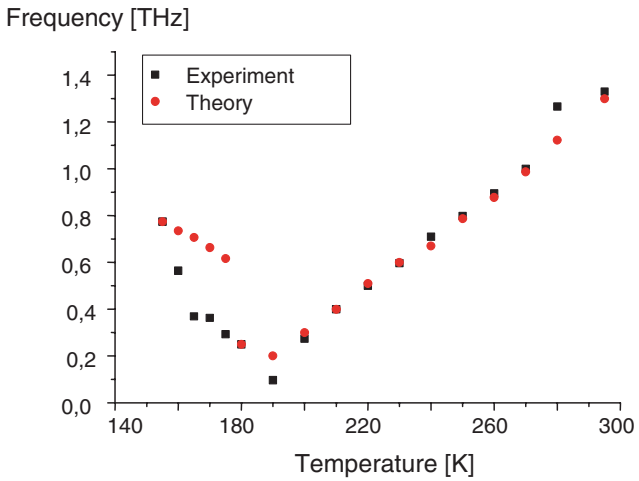

Figure 1. The temperature dependence of the soft zone boundary mode: squares refer to results of [8]; circles are theoretical results.

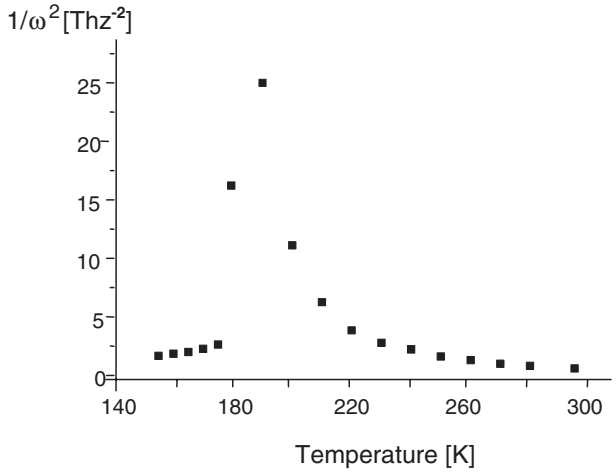

Figure 2. Calculated temperature-dependent scattering intensity proportional to $1/\omega^2$.

Table 1. Model parameters entering equation (1). The electron–phonon couplings g_2 , g_4 refer to the high-temperature phase. For $T < T_c$, both are a third of the values given in table. (Note: the signs of g_2 and g_4 are reversed as compared to the case for ferroelectrics, indicating the tendency towards delocalization of the Se p electrons and a local instability. This local instability does not reflect the overall crystalline stability which is preserved, as will be shown in another communication, where a double-well potential arises for temperatures $T > T_c$ and a broad single minimum potential for $T < T_c$.)

m_1 (10^{-22} g)	m_2 (10^{-22} g)	f (10^4 g s^{-2})	f' (10^4 g s^{-2})	g_2 (10^4 g s^{-2})	g_4 (10^{22} g s^{-2} cm^{-2})
2.662	0.4663	2.3875	0.4679	2.0313	−0.208

$$H = \sum_p \varepsilon_p c_p^+ c_p + \sum_q \hbar\omega_q b_q^+ b_q + \frac{1}{\sqrt{N}} \sum_{p,q} g_T(q) c_{p+q}^+ c_p (b_q + b_{-q}^+) \tag{5}$$

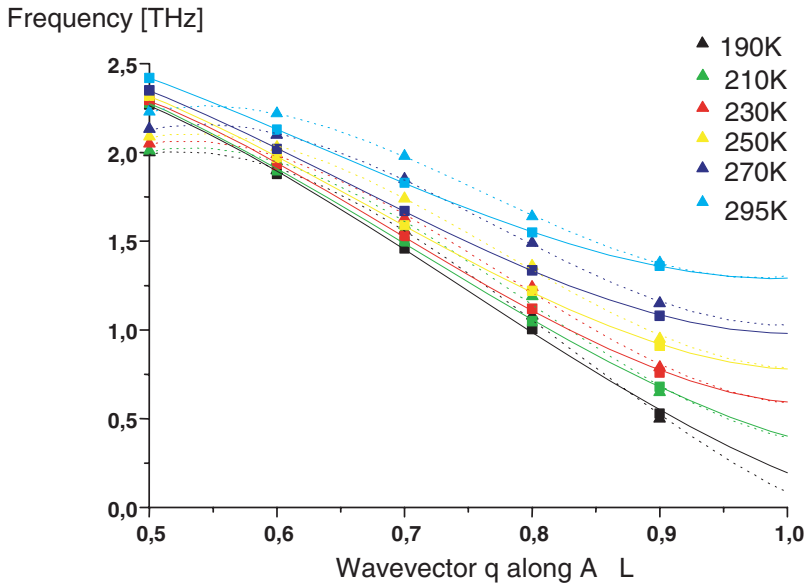

Figure 3. Comparison of the phonon dispersion curves of $TiSe_2$ as a function of temperature along the symmetry direction A–L from [8] (dotted curves and triangles) and the present calculations (full curves and squares)

where c, b are annihilation and creation operators for electrons with energy ε_p and transverse phonons with frequencies ω_q which are taken from the above calculations, as the electrons involved in the core–shell coupling are—for the above-given reasons—assumed to be the same ones as gave rise to the CDW formation. N is the number of unit cells in our pseudo-one-dimensional model. The important difference from various earlier models arises here from the fact that anharmonic terms are explicitly included. As will be shown below, these terms provide a natural explanation for the resistivity anomalies observed at the phase transition temperature [5] and explain the enormous redistribution of electronic band states with temperature which have been observed in photoemission experiments [21, 22]. Within equation (2) the CDW transition temperature T_c is given by $k_B T_c = 2.28\varepsilon_F \exp(-2\beta)$, where ε_F is the Fermi energy and 2β is the solution of [2]

$$2\beta = \varepsilon_F \int_{\Delta}^{\sqrt{(\varepsilon_F^2+\Delta^2)}} \mathrm{d}\varepsilon \, \frac{\tanh(\varepsilon/2k_BT)}{(\varepsilon^2-\Delta^2)^{1/2}(\varepsilon_F^2+\Delta^2-\varepsilon^2)^{1/2}} \tag{6}$$

where Δ is the phonon-induced gap and is proportional to g_T. Here Δ is related to the corresponding density-of-states function as follows:

$$N_c(\varepsilon) = N(0)\varepsilon_F|\varepsilon|(\varepsilon_F^2+\Delta^2-\varepsilon^2)^{-1/2}(\Delta^2-\varepsilon^2)^{-1/2} \tag{7}$$

which for $T = 0$ yields $\Delta(0) = 4\varepsilon_F \exp(-2\beta)$.

Equation (6) together with the T_c-defining equation and equation (7) are again solved self-consistently using the previously determined value of g_T, with no further adjustable parameter. Interestingly we find a strong temperature dependence of the Fermi energy which has a cusp at T_c (see figure 4) and is a strong indication of redistributions of electron densities at the Fermi level [21, 22] together with large changes in the effective free carrier mass which have been reported in [23]. It should be noted here that the absolute values of ε_F as derived from our analysis are unrealistically high, which we attribute to the approximation scheme used

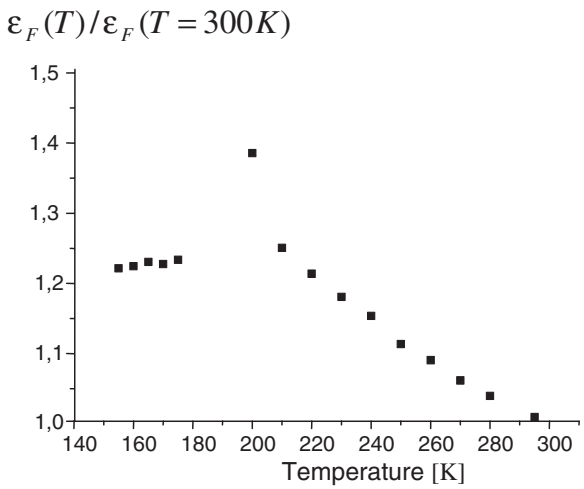

Figure 4. Relative change of the Fermi energy as a function of temperature.

in [2]. Consequently we show in figure 4 the relative variation of ε_F with temperature. The observed redistributions have, as a consequence, strong effects on the conductivity. As already noted above, strong anomalies have been reported in the resistivity in $TiSe_2$ around T_c [5] which have been interpreted as a strong temperature dependence of the carrier density where no explicit explanation could be offered for this effect. Here we can attribute the anomalies as arising from nonlinear electron–phonon interactions caused by a soft antiferroelectric zone boundary transverse optical mode. While there is a strong T-dependence of ε_F above T_c, this obviously vanishes below T_c and is indicative of the new CDW state. The zero-temperature CDW gap is derived from $\Delta(0) = 4\varepsilon_F \exp(-2\beta)$, is found to be 28 meV and exhibits a BCS-like temperature dependence. To our knowledge there are no experimental values available for the magnitude of the gap and we hope that our predictions will be verified soon.

In conclusion, we have shown that the microscopic origin of the CDW transition is the formation of an incipient antiferroelectric state which is driven by anharmonic electron–phonon interactions. Although we cannot rule out the occurrence of an actual antiferroelectric state induced by the p-electron polarizability, this state may be hidden by the CDW state and not easily detectable, but can clearly be indirectly inferred from dielectric constant anomalies [23]. The numerical calculations are based on a parameter-free self-consistent phonon approximation scheme and yield excellent agreement with many experimental data. Besides making explicit predictions for the CDW gap value, we also find strong evidence of anharmonic phonon-driven electronic redistributions with temperature which we consider to be the cause of the observed resistivity anomalies. Even though our calculations have been performed for the specific example of $TiSe_2$, we believe that antiferroelectrically driven CDW formation is common also to other compounds such as β-Na(Ag)V_2O_5, where antiferroelectric ordering of the intercalated cations is observed to precede a charge-ordering transition [24, 25]. Therefore we propose that an excitonic mechanism in the transition metal dichalcogenides can be ruled out. Since, to our knowledge, in the other members of the Ti dichalcogenide family, TiS_2 and $TiSe_2$, no anomalous phonon softening has been observed, we attribute this finding to the fact that a CDW instability is also not present.

References

[1] See, e.g.,
Gor'kov L P and Grüner G (ed) 1989 *Charge Density Waves in Solids* (New York: North-Holland)
Wilson J A and Yoffe A D 1969 *Adv. Phys.* **18** 193
[2] Rice M J and Strässler S 1973 *Solid State Commun.* **13** 125 and references therein
[3] Motizuki K (ed) 1986 *Structural Phase Transitions in Layered Transition Metal Compounds* (Boston, MA: Reidel)
[4] Di Salvo F J, Moncton D E, Wilson J A and Waszczak J V 1976 *Bull. Am. Phys. Soc.* **21** 261
[5] Di Salvo F J, Moncton D E and Waszczak J V 1976 *Phys. Rev.* B **14** 4321
[6] Stirling W G, Dorner B, Cheeke J D N and Revelli J 1976 *Solid State Commun.* **18** 931
[7] Wakabashi N, Smith H G, Woo K C and Brown F C 1978 *Solid State Commun.* **28** 923
[8] Holt M, Zschack P, Hong H, Chou M Y and Chiang T C 2001 *Phys. Rev. Lett.* **86** 3799
[9] Wilson J A 1978 *Phys. Status Solidi* b **86** 11
[10] White R M and Lucovsky G 1977 *Nuovo Cimento Soc. Ital. Fis.* B **38** 280
[11] Kohn W 1967 *Phys. Rev. Lett.* **19** 439
[12] Hughes H P 1977 *J. Phys. C: Solid State Phys.* **10** L319
[13] Jaswal S S 1979 *Phys. Rev.* B **20** 5297
[14] Migoni R, Bilz H and Bäuerle D 1976 *Phys. Rev. Lett.* **37** 1155
[15] Bilz H, Benedek G and Bussmann-Holder A 1987 *Phys. Rev.* B **35** 4840
[16] Bussmann-Holder A, Bilz H and Benedek G 1989 *Phys. Rev.* B **39** 9214
[17] Bussmann-Holder A and Büttner H 1992 *Nature* **360** 541
[18] Zunger A and Freeman A J 1978 *Phys. Rev. Lett.* **40** 1155
[19] Bussmann A, Bilz H, Roenspiess R and Schwarz K 1980 *Ferroelectrics* **25** 343
[20] Holy J A, Woo K C, Klein M V and Brown F C 1977 *Phys. Rev.* B **16** 3628
[21] Anderson O, Manzke R and Skibowski M 1985 *Phys. Rev. Lett.* **55** 2188
[22] Pillo Th, Hayoz J, Berger H, Lévy F, Schlapbach L and Aebi P 2000 *Phys. Rev.* B **61** 16 213
[23] Liang W Y, Lucovsky G, Mikkelsen J C and Friend R H 1979 *Phil. Mag.* B **39** 133
[24] Yamada H and Ueda Y 1999 *J. Phys. Soc. Japan* **68** 2735
[25] van Loosdrecht P 2001 private communication